Role of Mitochondrial Dynamics in Microglial Activation and Metabolic Switch

Alejandro Montilla
University of the Basque Country
Asier Ruiz
University of the Basque Country
Mar Marquez
University of the Basque Country
Amanda Sierra
University of the Basque Country
Carlos Matute
University of the Basque Country
Maria Domercq (maria.domercq@ehu.es)
University of the Basque Country

Research Article

Keywords: microglia, metabolic switch, pro-inflammatory stimul, Mdivi-1, mitochondria

Posted Date: January 6th, 2021

DOI: https://doi.org/10.21203/rs.3.rs-134161/v1

Role of mitochondrial dynamics in microglial activation and metabolic switch

Alejandro Montilla[1,2], Asier Ruiz[1,2], Mar Marquez[1], Amanda Sierra[1,3], Carlos Matute[1,2] and Maria Domercq[1,2]*

1- Achucarro Basque Center for Neuroscience and Department of Neuroscience, University of the Basque Country UPV/EHU, E-48940 Leioa, Spain
2- Centro de Investigación Biomédica en Red de Enfermedades Neurodegenerativas (CIBERNED), Leioa, Spain.
3- Ikerbasque Foundation, E-48009, Bilbao, Spain

***Correspondence should be addressed to**: María Domercq, Dpto. Neurociencias, Universidad del País Vasco, E-48940 Leioa, Spain. Tel: +34-94-6015681. Fax: +34-94-6015055. E-mail: maria.domercq@ehu.es

ABSTRACT

Microglia act as sensors of injury in the brain, favouring its homeostasis. Their activation and polarization towards a pro-inflammatory phenotype are associated to injury and disease. These processes are linked to a metabolic reprogramming of the cells, characterized by high rates of glycolysis and suppressed oxidative phosphorylation. This metabolic switch can be reproduced *in vitro* by microglial stimulation with lipopolysaccharide (LPS) plus interferon-γ (IFNγ). In order to understand the mechanisms regulating mitochondrial respiration abolishment, we examined potential alterations in mitochondrial features during this switch. Cells did not show any change in mitochondrial membrane potential, suggesting a limited impact in the mitochondrial viability. We provide evidence that reverse operation of F_0F_1-ATP synthase contributes to mitochondrial membrane potential. In addition, we studied the possible implication of mitochondrial dynamics in the metabolic switch using the mitochondrial division inhibitor-1 (Mdivi-1), which blocks Drp1-dependent mitochondrial fission. Mdivi-1 significantly reduced the expression of pro-inflammatory markers in LPS+IFNγ-treated microglia. However, this inhibition did not lead to a recovery of the oxidative phosphorylation ablation by LPS+IFNγ or to a microglia repolarization. Altogether, these results suggest that Drp1-dependent mitochondrial fission, although potentially involved in microglial activation, does not play an essential role in metabolic reprogramming and repolarization of microglia.

Keywords: microglia, metabolic switch, pro-inflammatory stimul, Mdivi-1, mitochondria

INTRODUCTION

Microglial cells are the resident macrophages of the central nervous system (CNS). They contribute to the tissue development, integrity and homeostasis through an active surveillance process [1,2] that can lead to different states of activation. Microglia display an enormous plasticity of responses to injury, ranging from effects that may contribute to neuroinflammation and eventually tissue damage, to essential responses for regenerative processes [3]. These mechanisms are associated to a broad spectrum of activation states, which are in turn related to molecular changes and adaptations [4]. One of these adaptive mechanisms is the metabolic reprogramming of microglia and other immune cells in response to immune activation [5–8]. Similar to macrophages [6,7], microglia exposed to pro-inflammatory stimulus shift their metabolism from oxidative phosphorylation (OXPHOS) to aerobic glycolysis [9,10], in an event similar to the Warburg effect suffered by cancer cells [7]. This metabolic reprogramming is essential to activate cellular defense mechanisms and to manage various microenvironments in inflamed tissue [7,11–13]. Moreover, these cells overexpress inflammatory markers such as interleukin-1β (IL-1β), tumour necrotic factor α (TNFα), or inducible nitric oxide synthase (iNOS), which takes part in the metabolism of arginine. In contrast, macrophages exposed to anti-inflammatory stimuli are primarily characterized by oxidative phosphorylation and increased fatty acid oxidation for ATP synthesis [6,12], a fact that has not been corroborated in microglia cells. This anti-inflammatory activation is commonly accompanied by an increase in the expression of specific markers, such as arginase 1 (Arg1), which competes with iNOS to hydrolyse arginine to ornithine [14], or the mannose receptor (MNR).

As mitochondria are crucial organelles in OXPHOS-related metabolism of the cells, we hypothesized that disbalances in their integrity or dynamics, may contribute to microglia metabolic reprogramming towards a glycolytic phenotype. Mitochondrial dynamics,

involving processes of both fusion and fission, are known to contribute to cell homeostasis and the maintenance of other mitochondrial functions [15]. Basal mitochondrial fission is required for mitochondrial trafficking to synapses, mitochondrial quality control, and brain development [16]. Misbalances in these dynamic mechanisms are thought to contribute to the development of various neurological disorders [17–19]. Moreover, these processes are associated to the production of reactive oxygen species (ROS). Mitochondrial fission is triggered by the dynamin-related protein 1 (Drp-1) recruitment from the cytosol to the outer mitochondrial membrane, which is mediated by different adaptor proteins [20,21]. Lately, the pharmacological inhibition of Drp1 with the mitochondrial division inhibitor 1 (Mdivi-1), a quinazonilone derivative, has become a promising strategy to analyse the physiological and pathological role of mitochondrial fission [22].

We tested whether mitochondria are functionally affected during metabolic reprogramming conditions. Moreover, we assessed whether mitochondrial fission is involved in microglia metabolic reprogramming. We used Mdivi-1 to block Drp1-dependent mitochondrial fission *in vitro*, and found that whereas this inhibition leads to a modulation of the expression of inflammatory markers in microglial cells, this is not sufficient to alter the metabolic switch suffered by the cells, in sharp contrast with the results reported in a previous study [9]. Furthermore, as Mdivi-1 treatment generated a decrease in iNOS expression, we have assessed whether this outcome was capable to favour a repolarization process in microglia.

MATERIALS AND METHODS

Animals

All experiments were performed according to the procedures approved by the Ethics Committee of the University of the Basque Country (UPV/EHU). Animals were handled in accordance with the European Communities Council Directive, and were kept under conventional housing conditions (22 ± 2°C, 55 ± 10% humidity, and 12-h day/night cycle) at the UPV/EHU animal facilities. The study was carried out in compliance with the ARRIVE guidelines. All possible efforts were made to minimize animal suffering and the number of animals used.

Microglial culture

Primary mixed glial cultures were prepared from the cerebral cortex of neonatal rats (P0-P2). After 10-15 days in culture, microglia were isolated by mechanical shaking (400 rpm, 1h) and purified by plating them on non-coated bacterial grade Petri dishes (Sterilin; Thermo Fisher), as previously described [23]. Microglial cells obtained with this procedure were cultured in Dulbecco's Modified Eagle Medium (DMEM; Gibco) supplemented with 10% Fetal Bovine Serum (FBS; Gibco).

Microglial cells were polarized with specific stimuli. To generate an anti-inflammatory phenotype in these cells, they were treated for 24 hours with IL-4 (20 ng/ml; Peprotech) and IL-13 (50 ng/ml; Peprotech). On the other hand, pro-inflammatory microglia were generated with a treatment of both LPS (10 ng/mL; Sigma-Aldrich) and IFNγ (20 ng/ml; Peprotech) 24 hours. In the experiments for the study of the pro-inflammatory activation time course, the LPS+IFNγ treatment was maintained for 2, 6 or 24 hours. The repolarization protocol implied a 24h pro-inflammatory activation followed by the treatment with the anti-inflammatory stimuli for the same amount of time.

106 **Immunofluorescence analysis**

107 Several immunocytochemistry (ICC) assays were performed on the cells in different
108 conditions. Cells in culture were fixed in 4% p-formaldehyde (PFA) in PBS and processed
109 for ICC as previously described [24]. Primary antibodies were used as follows to: Iba1
110 (1:500, Wako), iNOS (1:500, BD Bioscience), a pro-inflammatory marker, and mannose
111 receptor C type 1 (MRC1; 1:1000, Abcam), specific for anti-inflammatory cells. As
112 secondary antibodies, we used goat anti-rabbit Alexa Fluor 488 (1:250 Invitrogen) and
113 goat anti-mouse Alexa Fluor 594 (1:250, Invitrogen). The morphology of microglial cells
114 was analyzed using the Iba1 immunofluorescence, as the whole soma was stained by it.
115 The circularity of the cell was calculated as defined in the ImageJ software; a circular
116 shape would approach a value of 1. All the image analysis was performed with the ImageJ
117 software (NIH). Immunoreactivity of the different markers was calculated as the
118 fluorescence intensity normalized to the number of cells in the selected field of view.

119 **Cell viability assays**

120 Microglial viability was assessed using both the calcein-AM dye (Invitrogen) and the
121 Cytotox 96® Non-Radioactive Cytotoxicity Assay (Promega).

122 For the performance of the calcein assay, cells were incubated with 0.5 μM of the dye for
123 30 minutes at 37º C. The wells were then washed with PBS and the number of viable cells
124 were calculated with a Synergy HT fluorimeter/spectrophotometer reader (Bio-Tek) with
125 485 nm excitation and at 528 nm of emission wavelengths. A well with PBS was also
126 measured in each experiment to subtract its values as a background control. The results
127 are expressed as the relative percentage of cellular death with respect to non-treated
128 microglial cells.

For the Cytotox 96® Non-Radioactive Cytotoxicity Assay, culture supernatants were harvested from the plate, mixed with the specific Assay Buffer and incubated for 30 minutes at 37º C. The reaction was then stopped and the absorbance at 490 nm was immediately recorded in the fluorimeter. The levels of absorbance are associated with the amount of lactate dehydrogenase in the medium, a stable cytosolic enzyme that is released upon cellular death and its consequent lysis. All the data obtained through both assays was analysed using Gen5 software (Bio-Tek).

Quantitative RT-PCR

Total RNA of microglial cells was extracted using Trizol (Invitrogen) according to the manufacturer's instructions. Afterwards, 1 µg of this RNA was used to perform a retrotranscription protocol, using SuperScript III retrotranscriptase (200 U/µl; Invitrogen) and random hexamers as primers (Promega).

Real-time quantitative PCR reactions (qPCRs) were conducted in a Bio-Rad CFX96 real-time PCR detection system, as previously described [25]. The reactions were performed using SYBR-Green as a DNA-binding dye, and specific primers for anti-inflammatory and pro-inflammatory markers (Table 1). These primers were designed using Primer Express software (Applied Biosystems) at exon junctions to avoid genomic DNA amplification. The cycling conditions comprised 3 minutes of polymerase activation at 95°C and 40 cycles consisting of 10 seconds at 95°C and 30 seconds at 60ºC. After every qPCR reaction, the melting curve was assessed in order to check the specificity of the amplification. The amount of cDNA was quantified using a standard curve from a pool of cDNA obtained from the different conditions of each experiment. Subsequently, the results were normalized using a normalization factor, based on the geometric mean of housekeeping genes (Table 1), obtained for each condition using the GeNorm v3.5 software [26].

Mitochondrial membrane potential and mitochondrial calcium measurements

For quantification of mitochondrial membrane potential, microglial cells were loaded with quenching concentrations of Rhodamine 123 (Rh123; 10 µM) for 20 min in medium without phenol red. After this, microglia were washed for 10 minutes in the same medium. Living cell imaging was performed with a 63x objective in an inverted Leica LCS SP2-AOBS confocal microscope at an acquisition rate of 1 frame every 15 seconds for 5 min. After obtaining some basal images, FCCP (1 µM), an uncoupler of the mitochondrial oxidative phosphorylation, was added to the plates and the increase in the Rh123 fluorescence level was measured to determine the membrane potential. For each plate, a homogenous population of approximately 20 cells was selected in the field of view, and the background fluorescence signal was subtracted from the individual values.

For the measurement of the mitochondrial calcium content time-lapse images were acquired using a 63X objective in a Leica TCS STED CW SP8 confocal microscope, at an acquisition rate of 1 frame every 15 seconds for 5 min. Cells were loaded with 1 µM Fluo-4 (Thermo Fisher) in HBSS (Ca^{2+}- and Mg^{2+}-free) with 0.5 µM EGTA for 30 minutes at 37ºC. Subsequently, microglial cells were washed and after obtaining some basal images, 1 µM FCCP was added to depolarize the mitochondrial membrane and force the release of Ca^{2+} from mitochondrial matrix to the cytosol. The analysis was made as above.

Mitochondrial morphology analysis

For the quantification of mitochondrial length, living cell imaging was performed on microglial cells, loaded with Rhodamine 123 (Rh123; 50 nM) for 20 min. Mitochondrial images were taken using a Zeiss LSM800 confocal microscope at 40X magnification and a pixel resolution of 1024x1024, and analyzed using the Object Analyzer tool of Huygens

image analysis software (Scientific Volume Imaging, B.V, version 20.10). First, background noise was removed using the maximum fluorescence intensity value of Rhodamine 123 in the nuclear region. Afterwards, a size filter was applied to remove objects smaller than mitochondria (38 voxels = 0.06 μm^3) [27]. Next, a watershed segmentation was performed using a Sigma value of 0.2 to separate objects that were not discriminated in the raw images due to the inherent resolution limit of confocal microscopy. After this pre-processing, the average length of each mitochondrial object per cell was calculated.

Oxygen consumption rate analysis

Real time measurements of oxygen consumption rate (OCR), extracellular acidification rate (ECAR) and glycolytic proton efflux rate (glycoPER) were performed using a Seahorse XFe96 Extracellular Flux Analyzer (Agilent), following manufacturer's instructions to carry out the XF Cell Mito Stress Test Kit or the XF Glycolytic Rate Assay Kit (Agilent). Microglia cells were seeded as a monolayer in the XF96 microplate. Before the assay, cells were washed and equilibrated in the XF Assay modified DMEM medium for 30 minutes at 37ºC.

For the performance of the XF Cell Mito Stress Test Kit, the real levels of OCR were determined in response to the sequential addition of oligomycin (2 μM), FCCP (1 μM) and rotenone/antimycin A (0.5 μM). Specifically, basal mitochondrial respiration was calculated subtracting OCR rate after rotenone/antimycin A addition from basal OCR. as the last measurement before addition of oligomycin – non-mitochondrial respiration (minimum rate measurement after the treatment with rot/antA). The spare respiratory capacity was obtained by subtracting the basal respiration level from the maximum rate

measurement after addition of FCCP. ATP-linked OCR was determined by subtracting oligomycin-induced OCR from basal OCR.

For the measurement of the basal glycoPER, the XF Glycolytic Rate Assay Kit was carried out. This test includes the sequential addition of rotenone/antimycin A (0.5 μM), and 2-deoxyglucose (2-DG; 50 mM). The glycoPER corresponds to the proton efflux rate derived from glycolysis (discounting the effect of CO2-dependent acidification, included in the ECAR measurement) All these parameters were obtained using the specific Agilent Report Generator. For each single experiment, eight replicates were performed.

Data analysis

All the data shown in the figures are presented as the mean ± SEM. All the statistical analyses were performed with GraphPad Prism 8.0 (GraphPad Software, Inc.). Specifically, every comparison between two groups was analysed using paired Student's two-tailed t-test. Comparison among multiple groups were analysed by one-way analysis of variance (ANOVA) followed by Bonferroni's multiple comparison tests for *post hoc* analysis. Statistical significance was considered at $p < 0.05$.

RESULTS

Metabolic reprogramming in microglia is not associated to mitochondrial damage

To test whether microglia metabolic reprogramming from OXPHOS to glycolysis upon pro-inflammatory stimulation is associated to mitochondrial damage, we set up an *in vitro* protocol to study the metabolic switch and we measured oxygen consumption rate (OCR) and extracellular acidification rate (ECAR) in real time as indicative of mitochondrial respiration and glycolysis respectively. Cells treated with classical pro-inflammatory stimuli (LPS and IFNγ) showed a flat profile regarding OXPHOS, and all the parameters (basal OCR, ATP-linked respiration and spare respiratory capacity) related to this molecular process were practically abolished (Fig. 1A), as previously described [28]. This suggests a metabolism shift from OXPHOS to glycolysis in order to rapidly obtain energy. Conversely, microglia treated with anti-inflammatory factors (IL-4 and IL-13) showed a significant increase in basal OCR, spare respiratory capacity and ATP-linked respiration, thus, indicating that mitochondrial OXPHOS was boosted. In contrast, ECAR measurement showed an increase in basal glycolysis in both pro-inflammatory and anti-inflammatory microglia (Fig. 1B), suggesting that activated microglia have higher energetic demands. Moreover, inhibition of mitochondrial F_0F_1-ATP synthase with oligomycin, thus blocking OXPHOS, increased glycolytic rate in control and anti-inflammatory microglia but not in pro-inflammatory microglia (Fig. 1B). Finally, the basal ratio between mitochondria OCR (mitoOCR) and the glycolytic proton efflux rate (glycoPER) was significantly inhibited in pro-inflammatory microglia (Fig. 1C). These results further support the idea that pro-inflammatory microglia metabolism relies exclusively on glycolysis.

In other immune cells, such as dendritic cells, the metabolic switch to glycolysis occurs within minutes after TLR activation with LPS [29]. However, microglia acute treatment

with LPS did not induce any change in OCR (Fig. 1D). Time course analysis demonstrated that the metabolic switch began to occur at 2h, was clear at 6h and completed at 24h (Fig. 1E).

Since OXPHOS takes place in the mitochondrial inner membrane and it is determinant for H^+ movement and mitochondrial membrane potential ($\Delta\Psi m$) maintenance, the arrest of mitochondrial OXPHOS by pro-inflammatory stimuli could induce a collapse in $\Delta\Psi m$. To check whether mitochondrial membrane potential was altered in microglia treated with pro-inflammatory stimuli, we performed live cell imaging of Rhodamine 123 (Rh123) fluorescent dye in microglia under "quenching" conditions [30]. Addition of the mitochondrial oxidative phosphorylation uncoupler FCCP provoked the release of Rh123 from the mitochondria and consequently increased its cytoplasmic fluorescence two-fold over baseline (100%) in control microglia as well as in microglia treated with LPS + IFNγ (Fig. 2A), indicating that basal mitochondrial potential is maintained in pro-inflammatory microglia despite the arrest of OXPHOS. To further assess mitochondrial integrity we measured resting $[Ca^{2+}]_{mit}$ by recording $[Ca^{2+}]_{cyt}$ upon addition of FCCP in the absence of extracellular Ca^{2+}, which is indicative for $[Ca^{2+}]_{mit}$ [31]. Again, we observed no significant differences in the release of mitochondrial calcium to the cytosol after the addition of FCCP (Fig. 2B). Moreover, pro-inflammatory stimulation of microglia induced a significant increase in reactive oxygen species (ROS) production, as revealed with the dichlorofluorescein diacetate (DCFDA) dye (Fig. 2C), despite the blockage of OXPHOS. All these results suggest that pro-inflammatory activation and its subsequent lack of OXPHOS activity in microglia is not related to and it does induce any mitochondrial dysfunction or alteration in mitochondrial membrane potential.

Maintaining mitochondrial membrane potential is essential to prevent the release of pro-apoptotic factors into the cytosol and subsequent cell death. Indeed, despite the blockage

of OXPHOS, LPS plus IFNγ stimulation did not induce any significant microglia cell death (Fig. 2D). We hypothesized that ΔΨm could be maintained in cells with respiration inhibited by the reverse operation of F_0F_1-ATP synthase and the adenine nucleotide translocase (ANT), which pump H^+ out of the matrix [32]. To test this hypothesis, we analysed the impact of the F_0F_1-ATP synthase and ANT in cell viability and ΔΨm. Indeed, treatment of LPS + IFNγ stimulated microglia with oligomycin, a F_0F_1-ATP synthase inhibitor, induced a significant increase in microglia cell death (Fig. 2D). In contrast, bongkrekic acid, an inhibitor of ANT [33], did not induce microglia cell death (Fig. 2D). Accordingly, a role of F_0F_1-ATP synthase in mitochondrial ΔΨm maintenance in pro-inflammatory microglia was further corroborated by live cell imaging of tetramethylrhodamine ethyl ester (TMRE), a fluorescent dye that accumulates in active mitochondria. Addition of oligomycin induced a significant decrease in ΔΨm in pro-inflammatory microglia but not in control microglia (Fig. 2E), supporting the idea that the former's mitochondrial integrity depends on the activity of the ATP synthase.

Mitochondrial fission inhibition does not reverse mitochondrial metabolic reprogramming

Previous data have showed that activation of microglia with LPS induced a transient shortening of mitochondria by fission at 2h. Similarly, we detected a shortening of mitochondrial length at 2h after LPS + IFNγ treatment, an effect that was reverted in the presence of the mitochondrial fission inhibitor Mdivi-1 [9,34] (Figure S1). Since microglia metabolic switch has been associated previously to mitochondrial fission [9], we further analysed this hypothesis in our cultures using Mdivi-1. First, we assessed whether the Mdivi-1 treatment would have an effect on microglia itself. A 24h-treatment with Mdivi-

1 (50 µM) provoked a morphological change in microglia with a significant increase in cytoplasm circularity, indicating that Mdivi-1 treatment induces an amoeboid morphology (Fig. 3A). Although this characteristic is generally associated with cell activation, we found no differences in the basal expression of pro-inflammatory (iNOS) or anti-inflammatory markers (mannose receptor, MNR) (Fig. 3B), nor in cell viability (Fig. 3C). However, Mdivi-1 reduced significantly the increased expression of iNOS in response to LPS and IFNγ stimulation (Fig. 3D). We further analysed by qPCR the expression of different pro-inflammatory mediators. Treating microglia with LPS + IFN-γ induced an increase in all the pro-inflammatory genes expression assessed (*Ccl2, Il1b, iNOS)* with respect to control cells, and also the expression of arginase-1 (*Arg1*), an anti-inflammatory mediator which is known to carry an opposite function to iNOS regarding cellular metabolism [14]. The treatment with Mdivi-1 significantly reduced pro-inflammatory mediators overexpression as well as that of Arg1 (Fig. 3E). These results suggest that Drp1-dependent mitochondrial fission is potentially involved in microglial activation.

Next, we checked whether the impact of Mdivi-1 on microglial activation could affect microglia metabolic reprogramming. In addition to the blockage of drp-1 mitochondrial fission, Mdivi-1 could inhibit acutely and reversibly mitochondrial complex I in neurons [35]. To determine the direct impact of Mdivi-1 on microglial bioenergetics, we treated microglia with Mdivi-1 for 1h and 24h and we measured microglial OCR. We also observed a reduction in mitochondrial respiration at 1h, however the effect was transient and disappeared at 24h (Fig. 4A, B). Next, we analysed the impact of Mdivi-1 on the metabolic switch of pro-inflammatory microglia. Treatment with Mdivi-1 did not increase OCR levels in cells stimulated with LPS and IFNγ, to recover the normal bioenergetics profile (Fig. 4B). These results indicate that, although Drp1-mediated

mitochondrial fission could modulate or contribute to microglia activation, it does not play an active role in the metabolic switch produced in inflammatory paradigms.

Mdivi-1 treatment does not improve microglial repolarization

Redirection of microglia from a detrimental to a regenerative phenotype is a major concept to develop new therapies targeting these cells [36]. Nitric oxide (NO), the product of iNOS activity, blunts mitochondrial respiration of pro-inflammatory macrophages and this dysfunction prevents editing macrophage towards an anti-inflammatory phenotype. Thus, inhibiting NO production improves mitochondrial metabolic impairment and macrophages reprogramming towards an anti-inflammatory phenotype [37]. Given that Mdivi-1 reduced iNOS expression in pro-inflammatory microglia, we assessed the capacity of Mdivi-1 to promote repolarization in microglia. To that end, microglia cells were primed for 24 hours with LPS+IFNγ (with or without Mdivi-1, to reduce NO production), and then treated 24h with anti-inflammatory cytokines (see scheme on Fig. 5A). We first compared the IL-4+IL-13-induced response in cells previously primed with LPS+IFNγ with the response of cells exposed to anti-inflammatory stimulus only. After exposure to IL-4+IL-13, microglia primed with LPS+IFNγ exhibited efficient upregulation in the expression of the anti-inflammatory marker mannose receptor and downregulation in the expression of iNOS (Fig. 5B). The expression of iNOS and MNR were further reduced or increased respectively in cells treated with Mdivi-1 during LPS+IFNγ priming (Fig. 5B). When the metabolic profile of the cells was assessed using Seahorse XFe96 Analyzer, we observed that microglia primed with LPS+IFNγ recovered partially the mitochondrial respiration after exposure to IL-4+IL-13. However, Mdivi-1 treatment during LPS+IFNγ priming did not further enhance the final OCR and therefore

337 the OXPHOS activity (Fig. 5C). These results do not support the implication of
338 mitochondrial dynamics in the repolarization process of microglia.

339 **DISCUSSION**

340 Immunometabolism has recently emerged as an important focus of research, as it opens
341 a novel therapeutic approach for inflammatory and autoimmune diseases. To conduct
342 some responses, effector immune cells such as microglia/macrophages undergo a
343 metabolic reprogramming process [5,7]. Here, we have monitored this effect in primary
344 microglia and its consequences in mitochondrial integrity; moreover, we have checked
345 whether this metabolic switch is associated to mitochondrial fission. It is noteworthy to
346 mention that the ablation of oxidative phosphorylation in active cells is not due to a
347 challenge to mitochondrial integrity. Moreover, we have shown that Drp1-dependent
348 mitochondrial fission, although potentially involved in microglial activation, does not
349 play an essential role in metabolic reprogramming of microglia.

350 Upon pro-inflammatory stimulation, cells are able to redirect their entire metabolic
351 processes to the glycolytic pathway, in order to rapidly obtain energy. This process is an
352 outcome of different molecular pathways; nevertheless, the precise mechanisms involved
353 are yet to be defined. Here, we have observed that even though the oxidative
354 phosphorylation machinery is completely halted, this is not associated to mitochondrial
355 damage or dysfunction nor with microglia cell death. This is opposed to what was
356 observed when the Warburg effect was firstly described; he hypothesized that
357 dysfunctional mitochondria would be the reason underlying the switch in metabolism and
358 eventually, the development of cancer cells. [38]. Indeed, recent studies have highlighted
359 the importance of mitochondria regarding the production of ROS as agents to support not

only the development of cancer cells but also the pro-inflammatory state of macrophages [39,40]. Thus, toll like receptor activation in macrophages induced mitochondrial ROS generation, an essential step for efficient intracellular bacteria killing [40]. We observed that ΔΨm was maintained in pro-inflammatory microglia through the reverse operation of F_0F_1-ATP synthase and that this protects microglia from cell death. Indeed, the blockage of complex I, III and IV abolishes H^+ translocation and it would lead to a transient drop in ΔΨm. However, the F1 subunit of F_0F_1-ATP synthase can hydrolyse mitochondrial ATP under these circumstances and drives the F0-rotor to pump H^+ out of the matrix to be able to maintain the ΔΨm [41]. Thus, the mitochondria of pro-inflammatory microglia would become consumers, rather than ATP generators, further increasing the energetic demand of these cells [42]. We have not found any essential role in the ANT reversal activity, which has also been described as key in the ΔΨm maintenance process in similar paradigms [32].Signalling events mediated by extracellular signals can regulate the metabolic pathways in immune cells, such as macrophages or microglia [43]. Accordingly, diverse cellular functions have been associated to metabolic reprogramming, including those related to mitochondrial function in general. Previous data suggested that mitochondrial dynamics contribute to this mechanism [9]. Our results demonstrated that Mdivi-1, a mitochondrial fission inhibitor a putative division inhibitor, reduced the enhancement of markers associated to microglial activation after LPS and IFN-γ exposure. This effect on microglial activation is in agreement with other studies, even in other paradigms of treatment [9,34]. Drp1-mediated mitochondrial fission has been associated to enhanced activation of both p38 and NF-κβ, both mediators of signalling cascades leading to the expression of pro-inflammatory genes, in a paradigm of diabetic nephropathy [44]. Moreover, blocking Drp1-dephosphorylation with oleuropein reduced the production of pro-inflammatory factors in microglia as well [45]. In contrast, blockage of

385 mitochondrial fission with Mdivi-1 did not avoid the microglial metabolism switch to
386 glycolysis upon LPS+ IFN-γ exposure, nor did it provoke any effect in the control cells.
387 We concluded that mitochondria fission does not contribute to the metabolic switch in
388 microglia. This result is apparently at odd with previous results [9]. The contradiction may
389 be explained in the basis of the different paradigm used; in this study, microglia is
390 exposed to Mdivi-1 as a pre-treatment, before the stimulation with LPS.

391 Distinct arginine metabolism plays a key role in the metabolic plasticity of immune cells.
392 Pro-inflammatory microglia convert arginine into NO trough iNOS activity, increased in
393 this phenotype [14,46]. It has been described that the upregulation of iNOS and the resulting
394 generation of NO contributes to the impairment of mitochondrial respiration both in
395 immune cells as well as in astrocytes [47,48]. Moreover, editing macrophage and microglia
396 (re)polarization is emerging as a new therapeutic approach and iNOS have been described
397 as a target. Thus, iNOS inhibition improve metabolic and phenotypic reprograming to
398 anti-inflammatory macrophages [37]. Despite that Mdivi-1 treatment consistently reduced
399 iNOS expression in pro-inflammatory microglia as well as we did not detect any
400 significant improvement on mitochondrial respiration. There are two possible
401 interpretations. The complete blockage of iNOS activity and total abolishment of NO
402 production, as observed with the iNOS inhibitor 1400W , could be required to prevent the
403 metabolic switch [49]. In this sense, Mdivi-1 only partially reduced iNOS expression in pro-
404 inflammatory microglia. Alternatively, signalling pathways controlling metabolic switch
405 could differ from those regulating phenotypic and inflammatory expression. Indeed,
406 iNOS inhibition does not affect phenotypic polarization of cells, nor the inflammatory
407 cytokine secretion of macrophages [37]. Accordingly, the effect of Mdivi-1 on pro-
408 inflammatory gene expression does not produce any change on metabolism. For instance,
409 Mdivi-1 rapidly and reversible attenuated complex I-dependent reverse electron transfer-

410 mediated reactive oxygen species (ROS) production by brain mitochondria oxidizing
411 succinate [20].

412 **CONCLUSIONS**

413 In summary, the present study sheds some light into the role of mitochondria in the
414 metabolic reprogramming process in microglia. Pro-inflammatory stimuli dampen
415 mitochondrial function without compromising their integrity and our results point to F_0F_1-
416 ATP synthase as a key regulator of mitochondrial potential and cell viability maintenance
417 in these conditions. However, we concluded that mitochondrial dynamics, fusion-fission,
418 although potentially involved in pro-inflammatory gene expression, do not contribute to
419 microglial glycolytic switch after pro-inflammatory stimulation.

ACKNOWLEDGEMENTS

We kindly acknowledge the Microscopy Facilities of both the University of the Basque Country (UPV/EHU) and Achucarro Basque Center for Neuroscience for the technical support.

AUTHORS CONTRIBUTION

MD contributed to the conception and design of the study, data interpretation and manuscript writing. AM contributed to the data acquisition and analysis, data interpretation and manuscript writing. AR assisted to the data acquisition and interpretation. MM and AS contributed the analysis of mitochondrial morphology. CM substantially contributed to the revision of the work. All authors contributed to the manuscript revision, read, and approved the submitted version.

FUNDING

This work was supported by grants from Merck Serono (a business of Merck KGaA, Darmstadt, Germany); Spanish Ministry of Education and Science (SAF2016-75292-R); Spanish Ministry of Science and Innovation (PID2019-109724RB-I00), Basque Government (IT1203/19 and PI-2016-1-0016) and Centro de Investigación Biomédica en Red sobre Enfermedades Neurodegenerativas (CIBERNED; grant CB06/05/0076) to MD and CM. Also, it was supported by grants from Spanish Ministry of Science and Innovation with FEDER funds (RTI2018-099267-B- I00); Tatiana Foundation Project (P-048-FTPGB 201) and Basque Government (PIBA 2020_1_0030) to AS. AM and MM are predoctoral fellows of the Spanish Ministry of Education and Science and the University of the Basque Country EHU/UPV, respectively.

COMPETING INTERESTS STATEMENT

The authors declare no competing interests.

DATA AVAILABILITY

The datasets generated during and/or analysed during the current study are available from the corresponding author on reasonable request.

REFERENCES

1. Davalos, D. *et al.* ATP mediates rapid microglial response to local brain injury in vivo. *Nat. Neurosci.* **8**, 752–758 (2005).

2. Nimmerjahn, A., Kirchhoff, F. & Helmchen, F. Resting microglial cells are highly dynamic surveillants of brain parenchyma in vivo. *Science* **308**, 1314–1318 (2005).

3. Ransohoff, R. & El Khoury, J. Microglia in health and disease. *Cold Spring Harb Perspect Biol* **8** (2016).

4. Xue, J. *et al.* Transcriptome-Based Network Analysis Reveals a Spectrum Model of Human Macrophage Activation. *Immunity* **40**, 274–288 (2014).

5. Andrejeva, G. & Rathmell, J. C. Similarities and Distinctions of Cancer and Immune Metabolism in Inflammation and Tumors. *Cell Metab.* **26**, 49–70 (2017).

6. Stienstra, R., Netea-Maier, R. T., Riksen, N. P., Joosten, L. A. B. & Netea, M. G. Specific and Complex Reprogramming of Cellular Metabolism in Myeloid Cells during Innate Immune Responses. *Cell Metab.* **26**, 142–156 (2017).

7. Kelly, B. & O'Neill, L. A. J. Metabolic reprogramming in macrophages and dendritic cells in innate immunity. *Cell Res.* **25**, 771–784 (2015).

8. Lauro, C. & Limatola, C. Metabolic Reprograming of Microglia in the Regulation of the Innate Inflammatory Response. *Front Immunol.* **11**:493 (2020) doi:10.3389/fimmu.2020.00493.

9. Nair, S. *et al.* Lipopolysaccharide-induced alteration of mitochondrial morphology induces a metabolic shift in microglia modulating the inflammatory response in vitro and in vivo. *Glia* **67**, 1047–1061 (2019).

10. Hu, Y. *et al.* mTOR-mediated metabolic reprogramming shapes distinct microglia functions in response to lipopolysaccharide and ATP. *Glia* **68** 1031-1045 (2020)

11. Holland, R. *et al.* Inflammatory microglia are glycolytic and iron retentive and typify the microglia in APP/PS1 mice. *Brain. Behav. Immun.* **68**, 183–196 (2018).

12. Van den Bossche, J., O'Neill, L. A. & Menon, D. Macrophage Immunometabolism: Where Are We (Going)? *Trends Immunol.* **38**, 395–406 (2017).

13. Bernier, L. P., York, E. M. & MacVicar, B. A. Immunometabolism in the Brain: How Metabolism Shapes Microglial Function. *Trends Neurosci.* **43**, 854-869 (2020).

14. Rath, M., Müller, I., Kropf, P., Closs, E. I. & Munder, M. Metabolism via arginase or nitric oxide synthase : two competing arginine pathways in macrophages. *Front Immunol.* **5**:532 (2014).

15. Westermann, B. Mitochondrial fusion and fission in cell life and death. *Nat. Rev. Mol. Cell. Biol.* **11**, 872–884 (2010).

16. Ishihara, N. *et al.* Mitochondrial fission factor Drp1 is essential for embryonic development and synapse formation in mice. *Nat. Cell Biol.* **11**, 958–966 (2009).

17. Knott, A. B., Perkins, G., Schwarzenbacher, R. & Bossy-Wetzel, E. Mitochondrial Fragmentation in Neurodegeneration. *Nat Rev Neurosci* **9**, 505–518 (2008).

18. Cho, D. H., Nakamura, T. & Lipton, S. A. Mitochondrial dynamics in cell death and neurodegeneration. *Cell. Mol. Life Sci.* **67**, 3435–3447 (2010).

19. Reddy, P. *et al.* Dynamin-Related Protein 1 and Mitochondrial Fragmentation in Neurodegenerative Diseases. *Brain Res. Rev* **67**, 103–118 (2011).

20. Smirnova, E., Griparic, L., Shurland, D. & Bliek, A. M. Van Der. Dynamin-related Protein Drp1 Is Required for Mitochondrial Division in Mammalian Cells. *Mol. Biol. Cell* **12**, 2245–2256 (2001).

21. Fonseca, T. B., Sánchez-Guerrero, Á., Milosevic, I. & Raimundo, N. Mitochondrial fission requires DRP1 but not dynamins. *Nature* **570**, E34–E42 (2019).

22. Cassidy-stone, A. *et al.* Chemical inhibition of the mitochondrial division dynamin reveals its role in Bax/Bak-dependent mitochondrial outer membrane permeabilization. *Dev.Cell.* **14**, 193–204 (2008).

23. Domercq, M. *et al.* System xc- and Glutamate Transporter Inhibition Mediates Microglial Toxicity to Oligodendrocytes. *J. Immunol.* **178**, 6549–6556 (2007).

24. Domercq M, Sánchez-Gómez MV, Areso P. & Matute, C. Expression of glutamate transporters in rat optic nerve. *Eur J Neurosci* **11(7)**, 2226–36 (1999).

25. Domercq, M. *et al.* PET imaging with [18F]FSPG evidences the role of system xc- on brain inflammation following cerebral ischemia in rats. *Theranostics* **6**, 1753–1767 (2016).

26. Vandesompele, J. *et al.* Accurate normalization of real-time quantitative RT-PCR data by geometric averaging of multiple internal control genes. *Genome Biol.* **3** (2002) doi:10.1186/gb-2002-3-7-research0034.

504 27. Freya, T. G. & Mannellab, C. A. The internal structure of mitochondria. *Trends*
505 *Biochem. Sci.* **25**, 319-324 (2000).

506 28. Orihuela, R., McPherson, C. A. & Harry, G. J. Microglial M1/M2 polarization and
507 metabolic states. *Br. J. Pharmacol.* **173**, 649–665 (2016).

508 29. Everts, B. *et al.* TLR-driven early glycolytic reprogramming via the kinases TBK1-IKKε
509 supports the anabolic demands of dendritic cell activation. *Nat. Immunol.* **15**, 323–332
510 (2014).

511 30. Corona, J. C. & Duchen, M. R. Mitochondrial bioenergetics assessed by functional
512 fluorescence dyes. *Neuromethods* (2014) doi:10.1007/978-1-4939-1059-5_7.

513 31. Brocard, J. B., Tassetto, M. & Reynolds, I. J. Quantitative evaluation of mitochondrial
514 calcium content in rat cortical neurones following a glutamate stimulus. *J. Physiol.* **531**,
515 793–805 (2001).

516 32. Chinopoulos, C. Mitochondrial consumption of cytosolic ATP: Not so fast. *FEBS Lett.*
517 **585**, 1255–1259 (2011).

518 33. Henderson, P. J. & Lardy, H. A. Bongkrekic acid. An inhibitor of the adenine nucleotide
519 translocase of mitochondria. *J. Biol. Chem.* **245**, 1319-1326 (1970).

520 34. Katoh, M. *et al.* Polymorphic regulation of mitochondrial fission and fusion modifies
521 phenotypes of microglia in neuroinflammation. *Sci. Rep.* **7** (2017).

522 35. Bordt, E. A. *et al.* The Putative Drp1 Inhibitor mdivi-1 Is a Reversible Mitochondrial
523 Complex I Inhibitor that Modulates Reactive Oxygen Species. *Dev. Cell* **40**, 583-594.e6
524 (2017).

525 36. Fumagalli, M., Lombardi, M., Gressens, P. & Verderio, C. How to reprogram microglia
526 toward beneficial functions. *Glia* **66**, 2531–2549 (2018).

527 37. Van den Bossche, J. *et al.* Mitochondrial Dysfunction Prevents Repolarization of
528 Inflammatory Macrophages. *Cell Rep.* **17**, 684–696 (2016).

529 38. Warburg, O. On the origin of cancer cells. *Science* **123**, 309–314 (1956).

530 39. Porporato, P. E., Filigheddu, N., Pedro, J. M. B. S., Kroemer, G. & Galluzzi, L.
531 Mitochondrial metabolism and cancer. *Cell Res.* **28**, 265–280 (2018).

532 40. West, A. P. *et al.* TLR signalling augments macrophage bactericidal activity through
533 mitochondrial ROS. *Nature* **472**, 476–480 (2011).

534 41. Kinosita, K., Adachi, K. & Itoh, H. Rotation of F1-ATPase: How an ATP-driven

molecular machine may work. *Annu. Rev. Biophys. Biomol. Struct.* **33**, 245–268 (2004).

42. Solaini, G., Baracca, A., Lenaz, G. & Sgarbi, G. Hypoxia and mitochondrial oxidative metabolism. *Biochim. Biophys. Acta - Bioenerg.* **1797**, 1171–1177 (2010).

43. Wang, S. *et al.* Metabolic reprogramming of macrophages during infections and cancer. *Cancer Lett.* **452**, 14–22 (2019).

44. Zhang, L. *et al.* Inhibition to DRP1 translocation can mitigate p38 MAPK-signaling pathway activation in GMC induced by hyperglycemia. *Ren. Fail.* **37**, 903–910 (2015).

45. Park, J. *et al.* Anti-inflammatory effect of oleuropein on microglia through regulation of Drp1-dependent mitochondrial fission. *J. Neuroimmunol.* **306**, 46–52 (2017).

46. Yang, Z. & Ming, X. F. Functions of arginase isoforms in macrophage inflammatory responses: Impact on cardiovascular diseases and metabolic disorders. *Front. Immunol.* **5** (2014).

47. Everts, B. *et al.* Commitment to glycolysis sustains survival of NO-producing inflammatory dendritic cells. *Blood* **120**, 1422–1431 (2012).

48. Bolaños, J. P., Peuchen, S., Heales, S. J. R., Land, J. M. & Clark, J. B. Nitric Oxide-Mediated Inhibition of the Mitochondrial Respiratory Chain in Cultured Astrocytes. *J. Neurochem.* **63**, 910–916 (1994).

49. Garvey, E. P. *et al.* 1400W is a slow, tight binding, and highly selective inhibitor of inducible nitric-oxide synthase in vitro and in vivo. *J. Biol. Chem.* **272**, (1997).

554 **Table 1**

Target gene	**Forward** sequence **(5'->3')**	**Reverse** sequence **(5'->3')**
Arg1	GGATTGGCAAGGTGATGGAA	CGACATCAAAGCTCAGGTGAA
Ccl2	AGCAGCAGGTGTCCCAAA	TTCTTGGGGTCAGCACAGAC
Il1b	TGGCAACTGTTCCTGAACTCA	GGGTCCGTCAACTTCAAAGAAC
Nos2	GAGGAGCAGGTGGAAGACTA	GGAAAAGACTGCACCGAAGATA
Housekeeping gene	**Forward** sequence **(5'->3')**	**Reverse** sequence **(5'->3')**
Hprt2	CAGTACAGCCCCAAAATGGTTA	AGTCTGGCCTGTATCCAACA
Ppia	AGGGTTCCTCCTTTCACAGAA	TGCCGCCAGTGCCATTA

555 **Table 1. List of primers for quantitative real-time PCR.** Primers were designed using Primer
556 Express software (Applied Biosystems) at exon junctions to avoid genomic DNA amplification

FIGURES

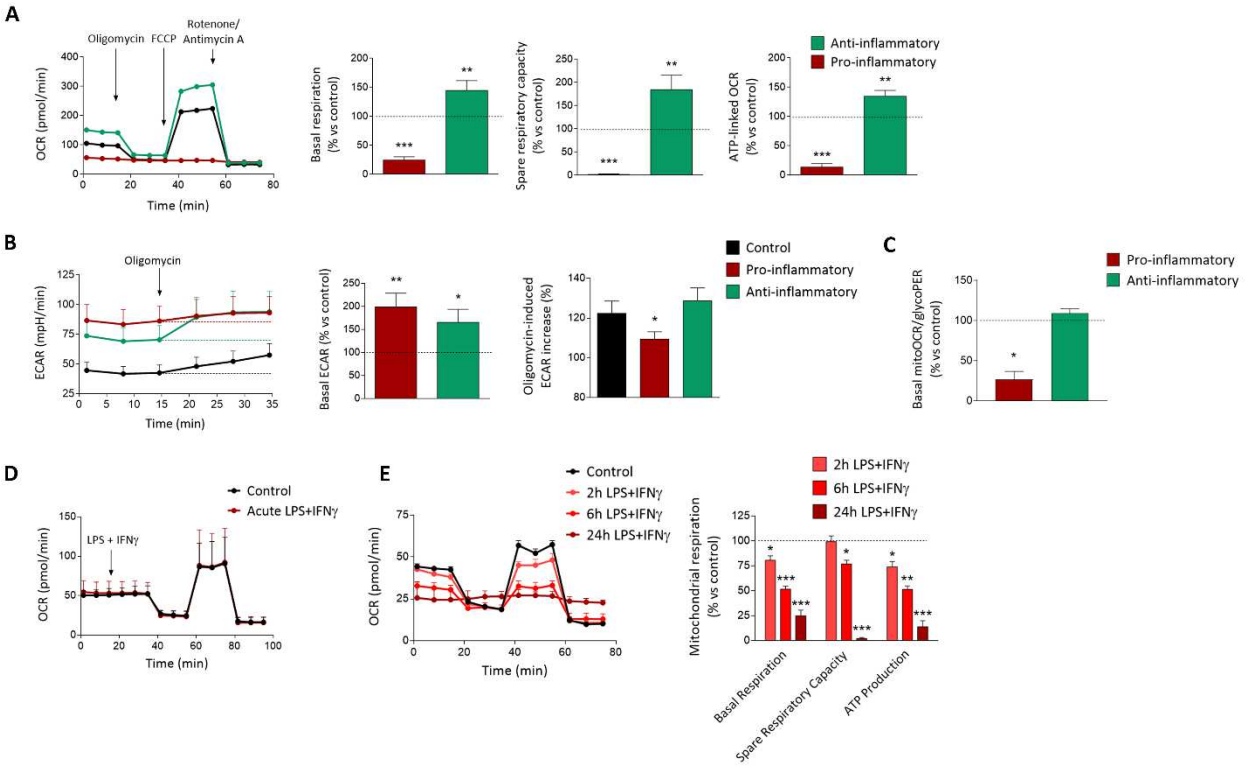

Figure 1. Robust metabolic reprogramming to glycolytic pathway after 24 hours of pro-inflammatory stimulation in microglia

(A) Representative experiment of OCR measurements in control microglia and in microglia after 24 hours of pro-inflammatory (LPS + IFNγ) and anti-inflammatory (IL-4 + IL-13) stimulations. Histograms show metabolic parameters obtained by the analysis of this metabolic profile compared to control cells (n = 7 independent experiments).

(B) ECAR measurement obtained by the secretion of lactate of control microglia and microglia after 24-hour incubation with pro- and anti-inflammatory factors (n = 7). Histograms show the basal level of this parameter as well as the increase provoked by the acute treatment with oligomycin, relative to the control cells. Statistical analysis was performed by one-way ANOVA followed by Bonferroni post-hoc test.

(C) Ratio between the basal OCR and the basal glycoPER control and both pro-inflammatory and anti-inflammatory microglia after 24 hours of stimulation. These parameters were obtained using the XF Glycolytic Rate Assay test (n = 3 independent experiments).

(D) Metabolic profile of microglia after acute treatment with LPS and IFNγ (n = 3)

(E) Metabolic profile of microglia treated during different time lapses with LPS and IFNγ. Histograms shows the metabolic parameters compared to control cells (n = 3).

Data are presented as means ± SEM. *p < 0.05, **p < 0.005, ***p < 0.001. Unless otherwise stated, Student's t-test was used to analyse the data.

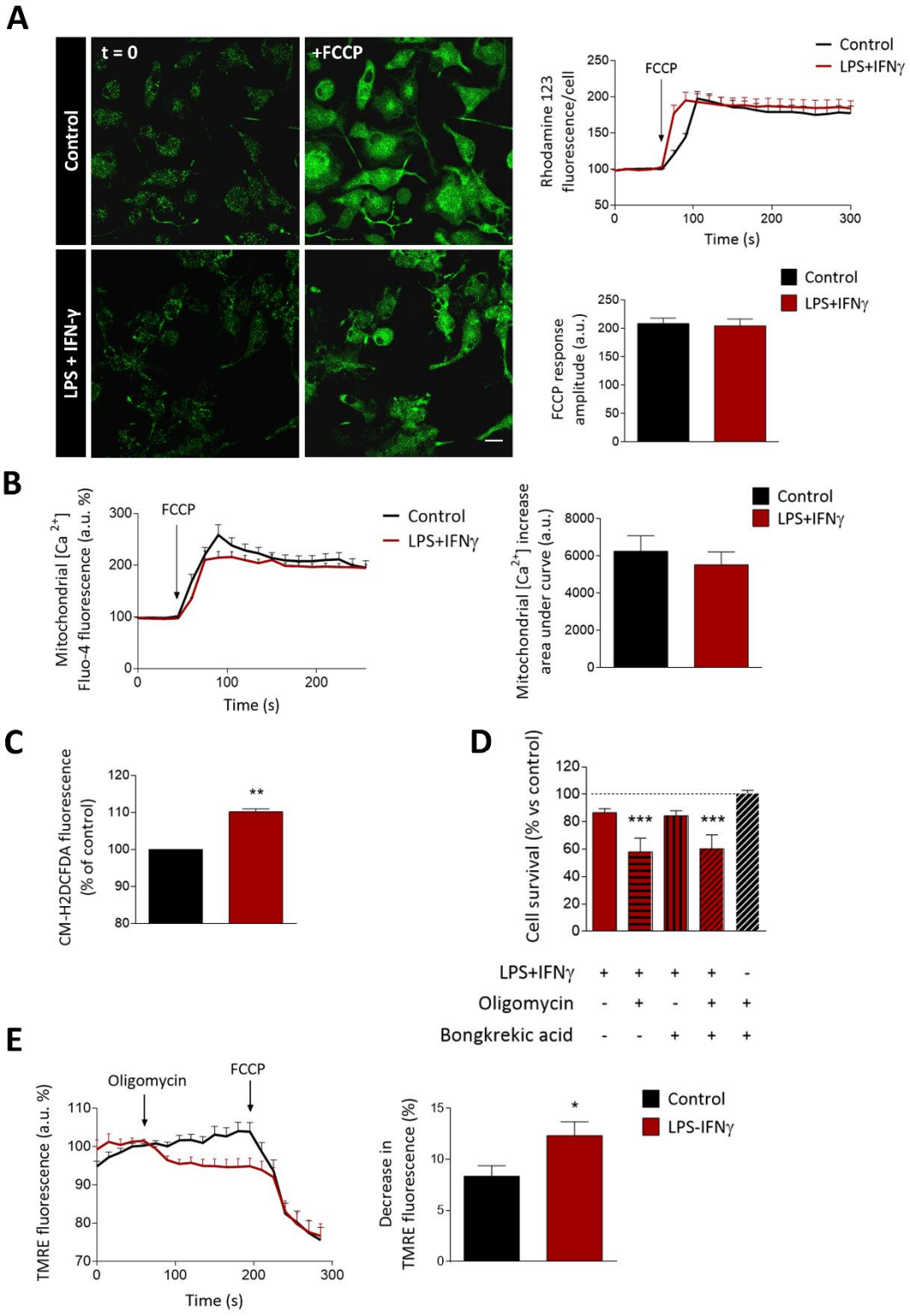

Figure 2. Pro-inflammatory microglia maintain mitochondrial integrity upon ATPase activity blockade

(A) Measurement of mitochondrial potential, represented as the increase in cytoplasmic Rh123 fluorescence measured after acute exposure to FCCP in control and LPS+IFNγ treated microglia (n = 50-75 cells from three independent experiments).

(B) Measurement of mitochondrial-specific calcium represented as the increase in cytoplasmic Fluo-4 fluorescence in a Ca^{2+}-free medium, after exposure to FCCP, in control and LPS+IFNγ treated cells (n = 50-75 cells from three independent experiments).

(C) Reactive oxygen species quantification in control and pro-inflammatory cells (n = 3 experiments performed in triplicate).

(D) Microglial viability after 24-hour treatment with LPS+IFNγ, oligomycin and/or bongkrekic acid, compared to control cells. One-way ANOVA followed by Bonferroni post-hoc analysis (n = 3 experiments performed in triplicate).

(E) Effect of ATPase inhibitor oligomycin in mitochondrial potential of control and LPS+IFN-γ treated cells (n = 70-80 cells from three independent experiments).

Data are presented as means ± SEM. *p < 0.05, **p < 0.005, ***p < 0.001. Unless otherwise stated, Student's t-test was used to analyze the data.

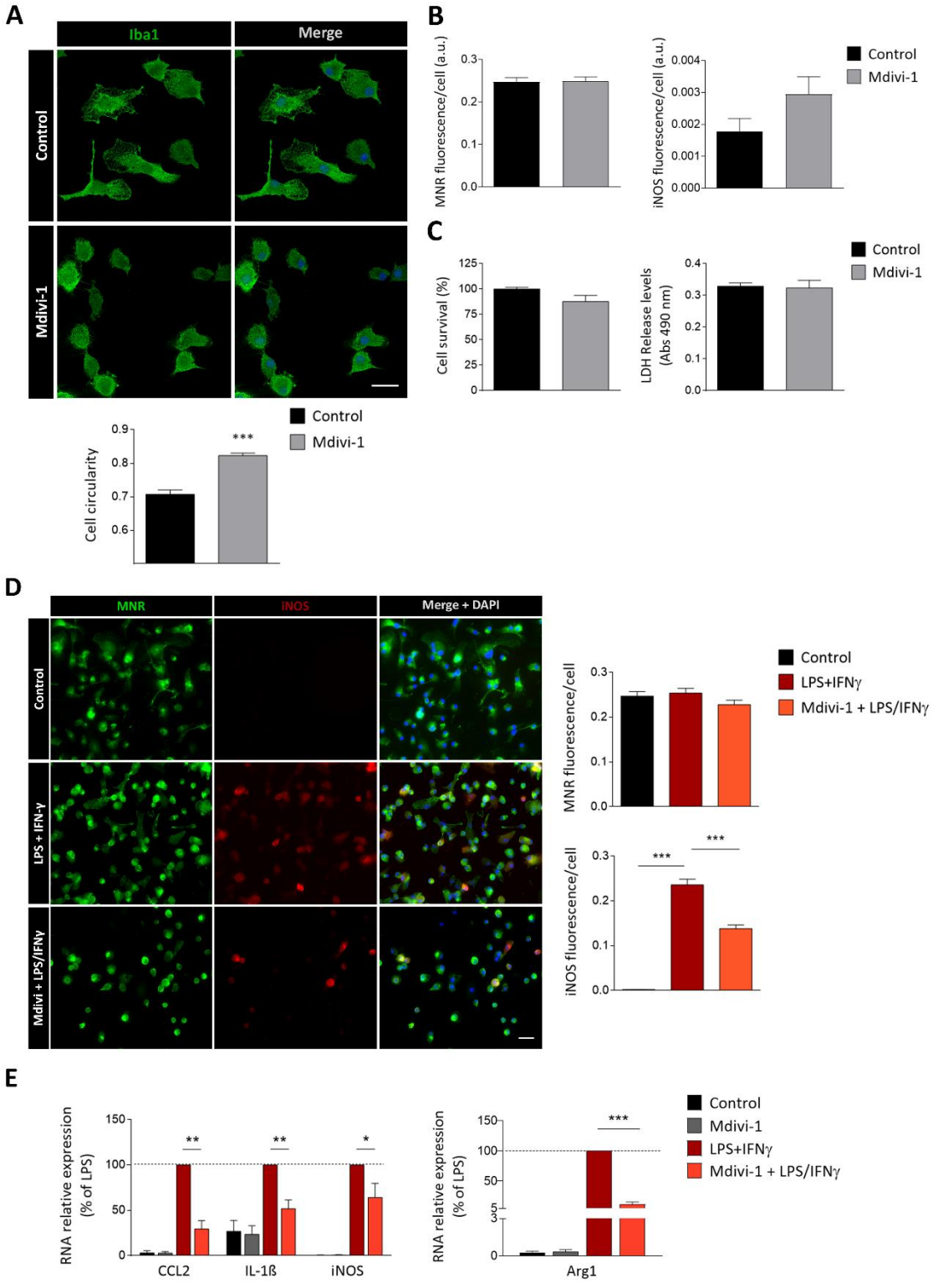

598

599 **Figure 3. Mitochondrial fission inhibition reduces the microglial inflammatory**
600 **markers**

(A) Representative images of Iba1$^+$ control and Mdivi-1 treated microglia. Right column shows Iba1$^+$ and DAPI staining (merge). Scale bar = 25 µm. Histogram represents the circularity of the cells as calculated by ImageJ software (n = 200 cells from three independent experiments).

(B) Expression of anti-inflammatory (MNR) and pro-inflammatory mediators (iNOS) in control and Mdivi-1 treated microglia (n = 4 independent experiments performed with duplicates).

(C) Microglial viability in control and Mdivi-1 cells, measured by both calcein assay and the quantification of LDH release to the medium, indicative of cell death (n = 3 experiments performed in triplicate).

(D) Representative immunostaining of MNR and iNOS in control microglia, as well as in cells treated with LPS+IFNγ or Mdivi-1 and LPS+IFNγ. Scale bar = 40 µm. Histograms represent the mean fluorescence of the staining per cell (n = 4 independent experiments performed with duplicates). One-way ANOVA followed by Bonferroni post-hoc analysis.

(E) Quantitative real time PCR (qRT-PCR) of pro-inflammatory (left) and an anti-inflammatory mediators (right) in control microglia, as well as in microglia treated with Mdivi-1, LPS+IFNγ, and Mdivi-1 + LPS+IFNγ (n = 4 experiments performed in duplicate). Data are expressed relative to the expression in LPS+IFNγ. One-way ANOVA followed by Bonferroni post-hoc analysis.

Data are presented as means ± SEM. *$p < 0.05$, **$p < 0.005$, ***$p < 0.001$. Unless otherwise stated, Student's t-test was used to analyze the data.

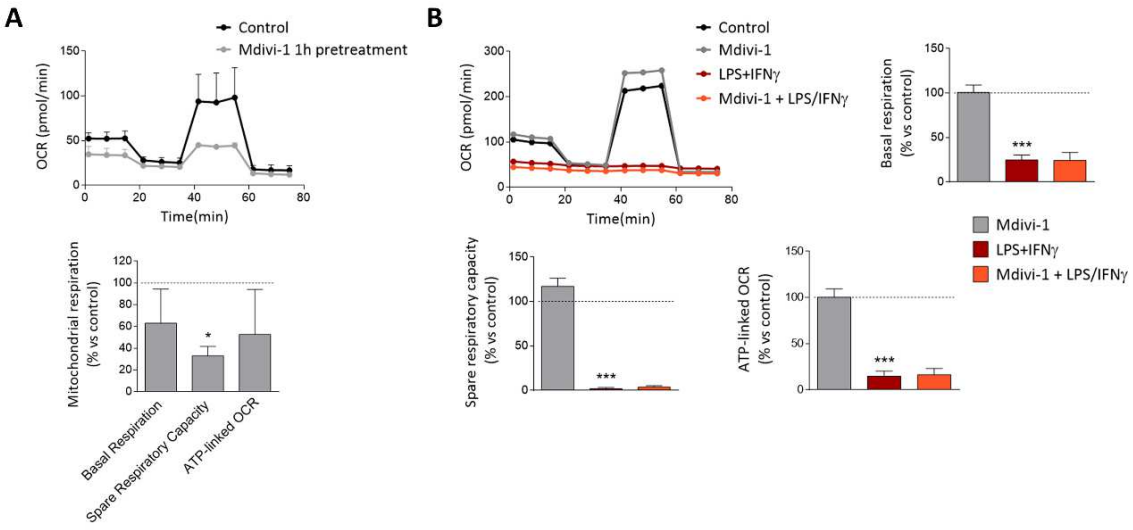

Figure 4. Mitochondrial fission inhibition does not reverse mitochondrial metabolic reprogramming

(A) Metabolic profile of control and microglia treated for 1 hour with Mdivi-1 (above). Histogram shows the metabolic parameters related to OCR of Mdivi-1 treated cells, compared to the control ones (n = 3).

(B) Metabolic profile of control microglia, as well as microglia treated for 24 hours with Mdivi-1, LPS+IFNγ and Mdivi-1 + LPS+IFNγ. Histograms show the metabolic parameters related to OCR compared to control microglia (n = 3).

Data are presented as means ± SEM. *p < 0.05, ***p < 0.001. One-way ANOVA followed by Bonferroni post-hoc analysis.

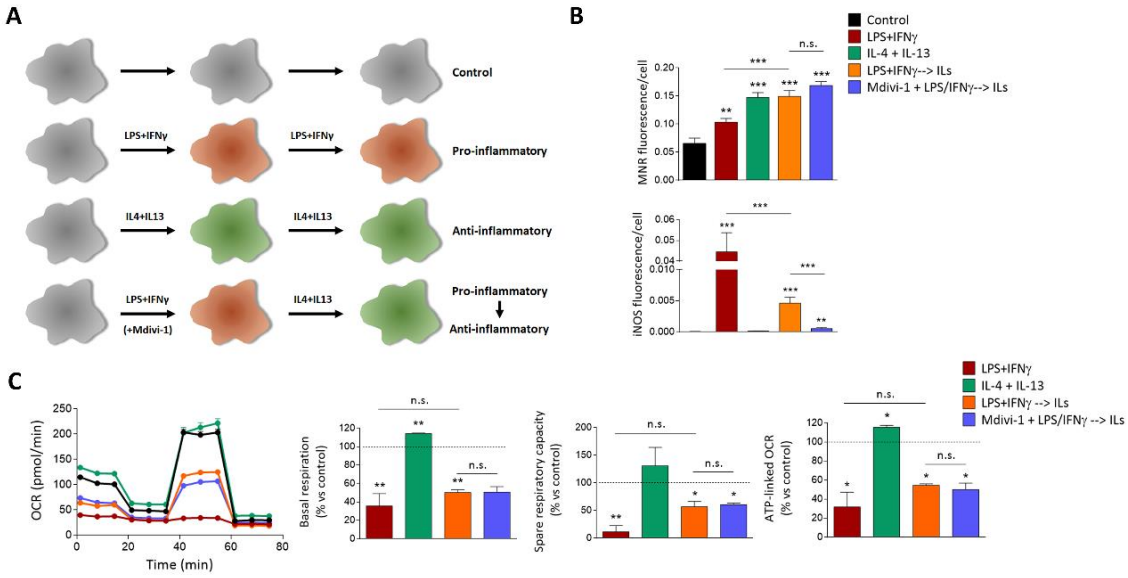

636 **Figure 5. Mdivi-1 treatment does not promote microglial repolarization**

637 (A) Scheme of the conditions used to study the role of Mdivi-1 in the repolarization capacity
638 of microglia. Each treatment indicated lasts 24 hours. Anti-inflammatory microglia (ILs-
639 treated) were compared to microglia that were primed for 24 hr with LPS + IFNγ before
640 24 hr treatment with ILs.
641 (B) Expression of anti-inflammatory (MRC1) and pro-inflammatory (iNOS) markers in every
642 condition of the repolarization experiment. Histograms represent the mean ± s.e.m of the
643 marker fluorescence intensity per cell (n =3 experiments performed in triplicate).
644 (C) Metabolic profile (left) of microglia treated as schematized in subfigure A. Histograms
645 (right) show metabolic parameters regarding OCR of the cells (n =3). Data was expressed
646 as fold change versus control non-treated microglia.

647 Data are presented as means ± SEM. *p < 0.05, **p < 0.005, ***p < 0.001. Student's t-test.

Figures

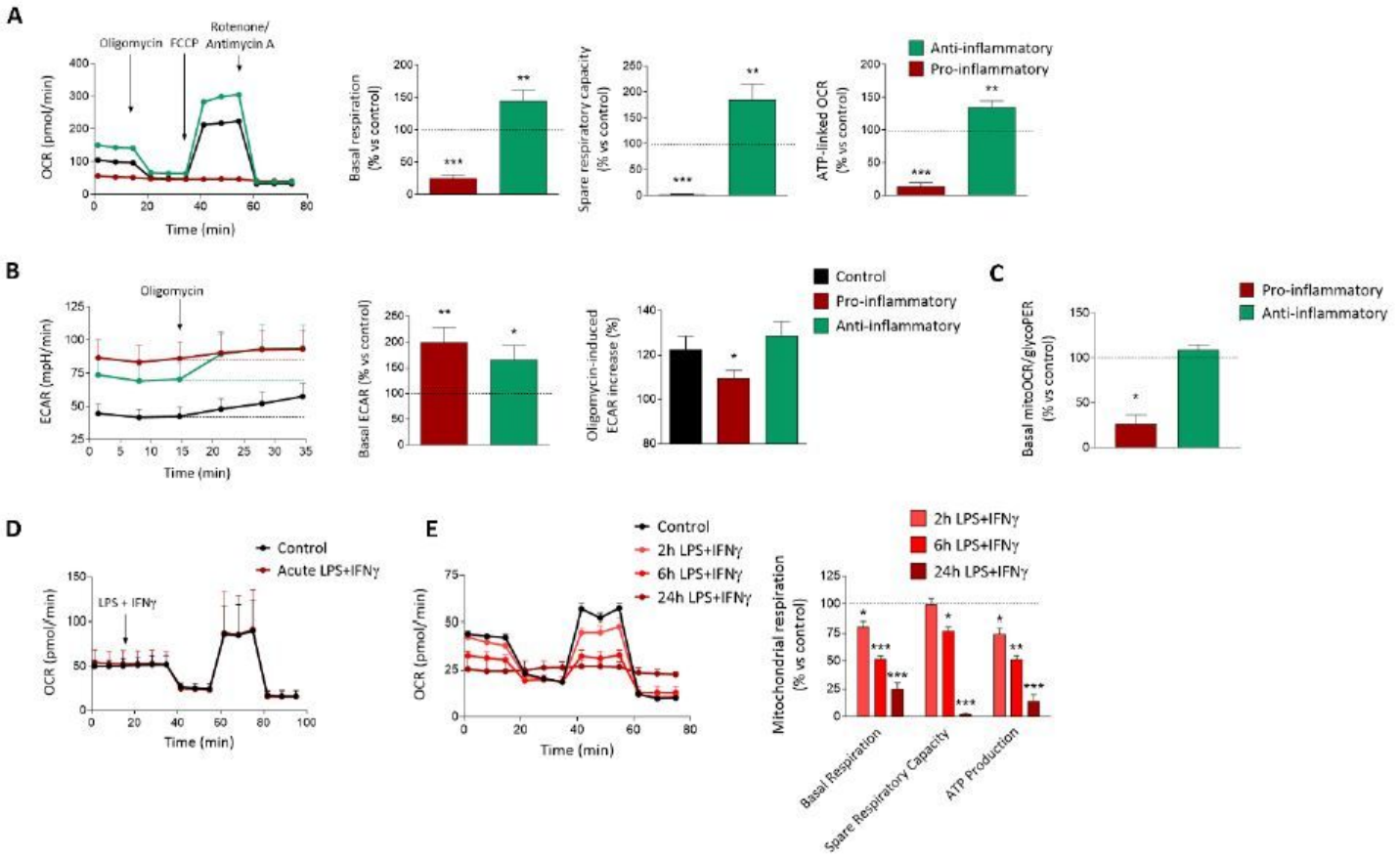

Figure 1

Robust metabolic reprogramming to glycolytic pathway after 24 hours of pro-inflammatory stimulation in microglia (A) Representative experiment of OCR measurements in control microglia and in microglia after 24 hours of pro-inflammatory (LPS + IFNγ) and anti-inflammatory (IL-4 + IL-13) stimulations. Histograms show metabolic parameters obtained by the analysis of this metabolic profile compared to control cells (n = 7 independent experiments). (B) ECAR measurement obtained by the secretion of lactate of control microglia and microglia after 24-hour incubation with pro- and anti-inflammatory factors (n = 7). Histograms show the basal level of this parameter as well as the increase provoked by the acute treatment with oligomycin, relative to the control cells. Statistical analysis was performed by one-way ANOVA followed by Bonferroni post-hoc test. (C) Ratio between the basal OCR and the basal glycoPER control and both pro-inflammatory and anti-inflammatory microglia after 24 hours of stimulation. These parameters were obtained using the XF Glycolytic Rate Assay test (n = 3 independent experiments). (D) Metabolic profile of microglia after acute treatment with LPS and IFNγ (n = 3) (E) Metabolic profile of microglia treated during different time lapses with LPS and IFNγ. Histograms shows the metabolic parameters compared to control cells (n = 3). Data are presented as means ± SEM. *p < 0.05, **p < 0.005, ***p < 0.001. Unless otherwise stated, Student's t-test was used to analyse the data.

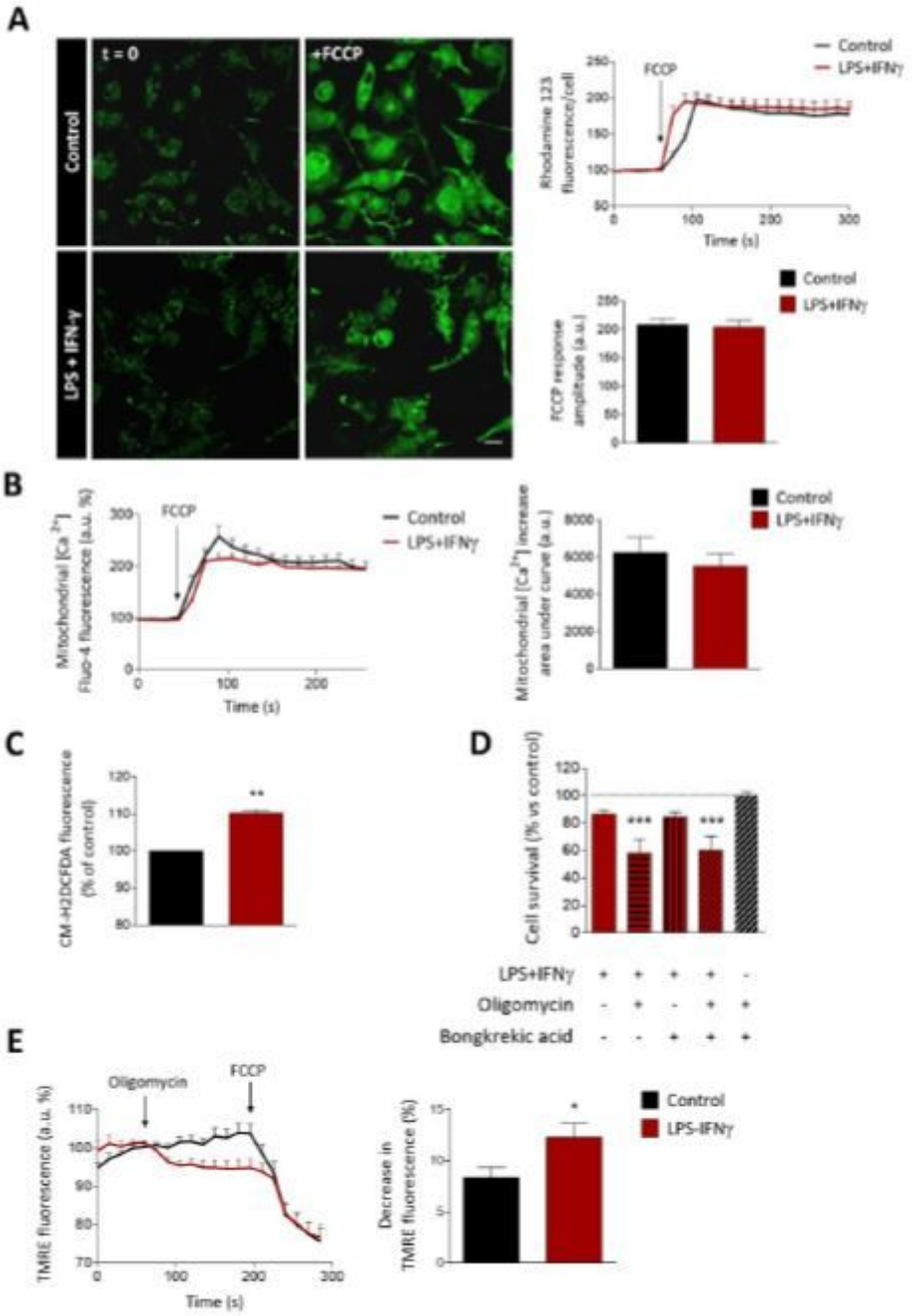

Figure 2

Pro-inflammatory microglia maintain mitochondrial integrity upon ATPase activity blockade (A) Measurement of mitochondrial potential, represented as the increase in cytoplasmic Rh123 fluorescence measured after acute exposure to FCCP in control and LPS+IFNγ treated microglia (n = 50-75 cells from three independent experiments). (B) Measurement of mitochondrial-specific calcium represented as the increase in cytoplasmic Fluo-4 fluorescence in a Ca2+-free medium, after exposure to FCCP, in control and LPS+IFNγ treated cells (n = 50-75 cells from three independent experiments). (C) Reactive oxygen species quantification in control and pro-inflammatory cells (n = 3 experiments performed in triplicate). (D) Microglial viability after 24-hour treatment with LPS+IFNγ, oligomycin and/or bongkrekic acid, compared

to control cells. One-way ANOVA followed by Bonferroni post-hoc analysis (n = 3 experiments performed in triplicate). (E) Effect of ATPase inhibitor oligomycin in mitochondrial potential of control and LPS+IFN-γ treated cells (n = 70-80 cells from three independent experiments). Data are presented as means ± SEM. *p < 0.05, **p < 0.005, ***p < 0.001. Unless otherwise stated, Student's t-test was used to analyze the data.

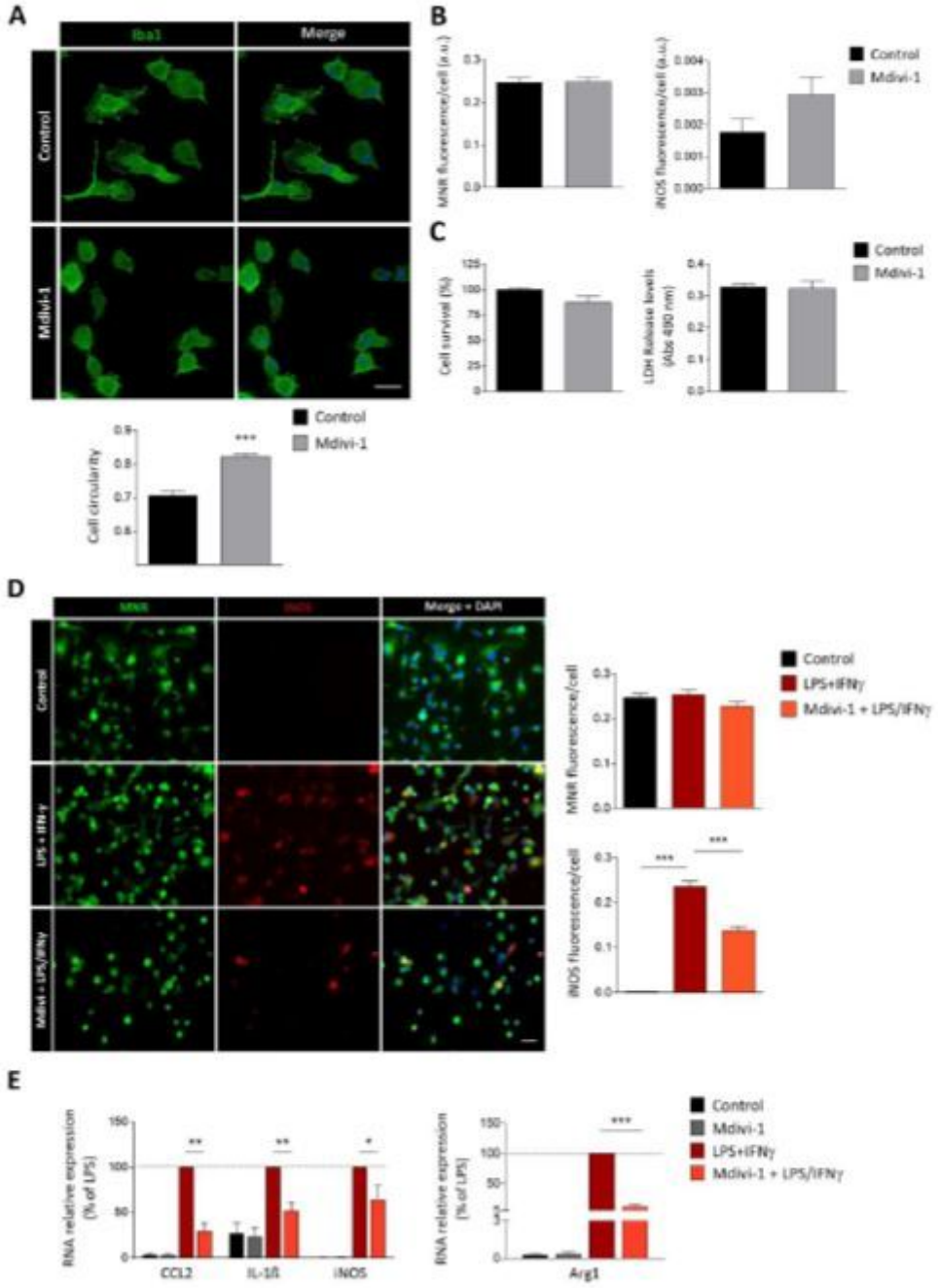

Figure 3

Mitochondrial fission inhibition reduces the microglial inflammatory markers (A) Representative images of Iba1+ control and Mdivi-1 treated microglia. Right column shows Iba1+ and DAPI staining (merge). Scale bar = 25 μm. Histogram represents the circularity of the cells as calculated by ImageJ software (n = 200 cells from three independent experiments). (B) Expression of anti-inflammatory (MNR) and pro-

inflammatory mediators (iNOS) in control and Mdivi-1 treated microglia (n = 4 independent experiments performed with duplicates). (C) Microglial viability in control and Mdivi-1 cells, measured by both calcein assay and the quantification of LDH release to the medium, indicative of cell death (n = 3 experiments performed in triplicate). (D) Representative immunostaining of MNR and iNOS in control microglia, as well as in cells treated with LPS+IFNγ or Mdivi-1 and LPS+IFNγ. Scale bar = 40 μm. Histograms represent the mean fluorescence of the staining per cell (n = 4 independent experiments performed with duplicates). One-way ANOVA followed by Bonferroni post-hoc analysis. (E) Quantitative real time PCR (qRT-PCR) of pro-inflammatory (left) and an anti-inflammatory mediators (right) in control microglia, as well as in microglia treated with Mdivi-1, LPS+IFNγ, and Mdivi-1 + LPS+IFNγ (n = 4 experiments performed in duplicate). Data are expressed relative to the expression in LPS+IFNγ. One-way ANOVA followed by Bonferroni post-hoc analysis. Data are presented as means ± SEM. *p < 0.05, **p < 0.005, ***p < 0.001. Unless otherwise stated, Student's t-test was used to analyze the data.

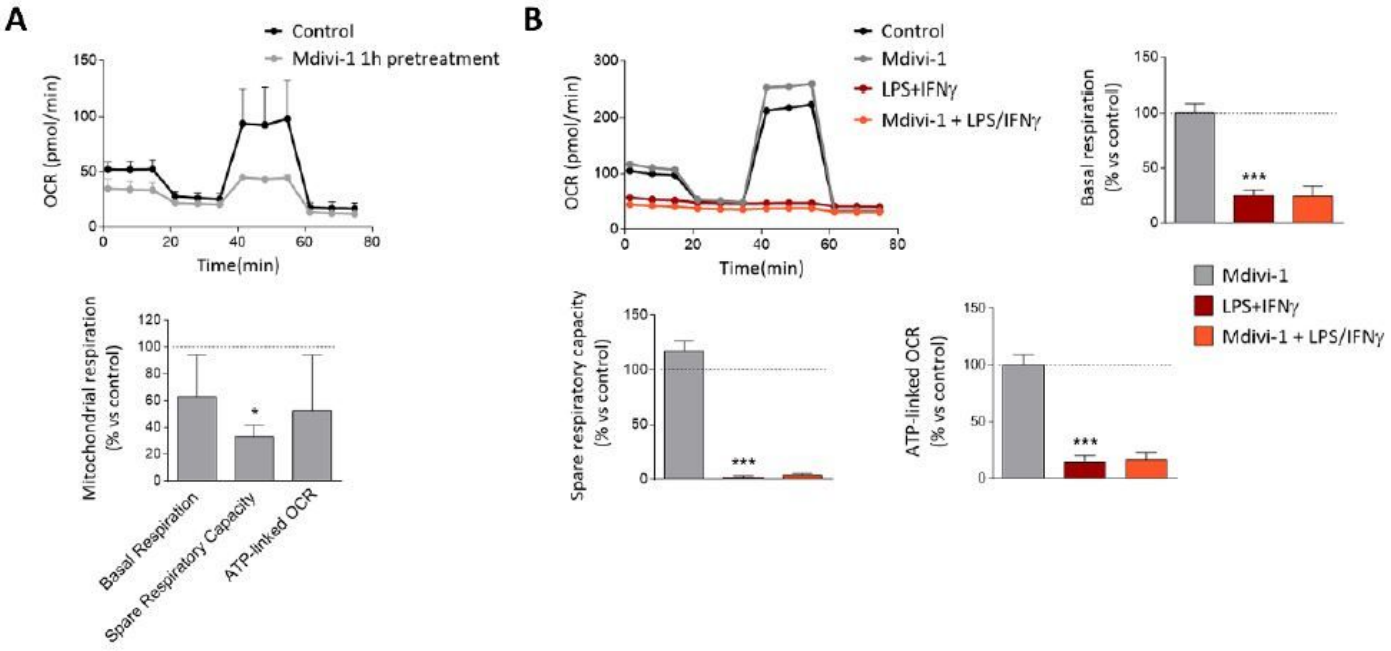

Figure 4

Mitochondrial fission inhibition does not reverse mitochondrial metabolic reprogramming (A) Metabolic profile of control and microglia treated for 1 hour with Mdivi-1 (above). Histogram shows the metabolic parameters related to OCR of Mdivi-1 treated cells, compared to the control ones (n = 3). (B) Metabolic profile of control microglia, as well as microglia treated for 24 hours with Mdivi-1, LPS+IFNγ and Mdivi-1 + LPS+IFNγ. Histograms show the metabolic parameters related to OCR compared to control microglia (n = 3). Data are presented as means ± SEM. *p < 0.05, ***p < 0.001. One-way ANOVA followed by Bonferroni post-hoc analysis.

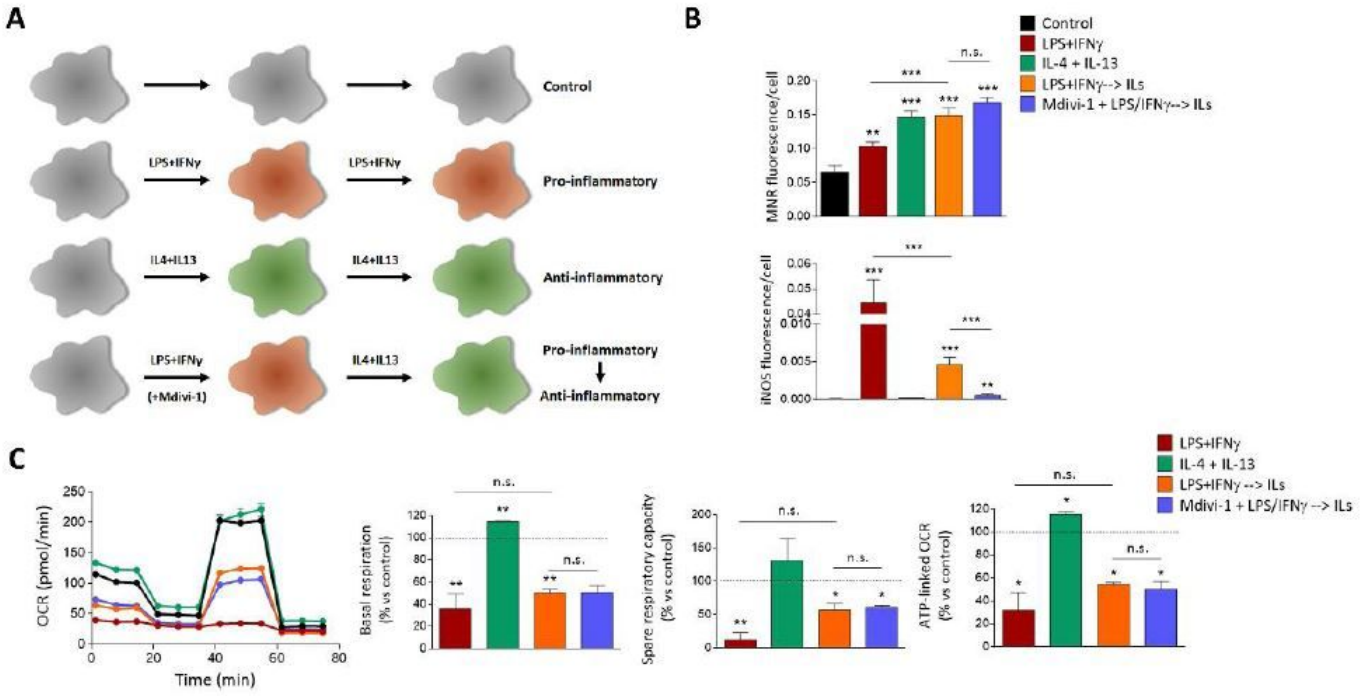

Figure 5

Mdivi-1 treatment does not promote microglial repolarization (A) Scheme of the conditions used to study the role of Mdivi-1 in the repolarization capacity of microglia. Each treatment indicated lasts 24 hours. Anti-inflammatory microglia (ILs- treated) were compared to microglia that were primed for 24 hr with LPS + IFNγ before 24 hr treatment with ILs. (B) Expression of anti-inflammatory (MRC1) and pro-inflammatory (iNOS) markers in every condition of the repolarization experiment. Histograms represent the mean ± s.e.m of the marker fluorescence intensity per cell (n =3 experiments performed in triplicate). (C) Metabolic profile (left) of microglia treated as schematized in subfigure A. Histograms (right) show metabolic parameters regarding OCR of the cells (n =3). Data was expressed as fold change versus control non-treated microglia. Data are presented as means ± SEM. *p < 0.05, **p < 0.005, ***p < 0.001. Student's t-test.

Supplementary Files

This is a list of supplementary files associated with this preprint. Click to download.

- Supplementarymaterial.docx